OPEN ACCESS Freely available online

PLoS one

Lobe-Specific Calcium Binding in Calmodulin Regulates Endothelial Nitric Oxide Synthase Activation

Pei-Rung Wu, Cheng-Chin Kuo, Shaw-Fang Yet, Jun-Yang Liou, Kenneth K. Wu*, Pei-Feng Chen*

Institute of Cellular and System Medicine, National Health Research Institutes, Zhunan, Miaoli County, Taiwan

Abstract

Background: Human endothelial nitric oxide synthase (eNOS) requires calcium-bound calmodulin (CaM) for electron transfer but the detailed mechanism remains unclear.

Methodology/Principal Findings: Using a series of CaM mutants with E to Q substitution at the four calcium-binding sites, we found that single mutation at any calcium-binding site (B1Q, B2Q, B3Q and B4Q) resulted in ~2–3 fold increase in the CaM concentration necessary for half-maximal activation (EC50) of citrulline formation, indicating that each calcium-binding site of CaM contributed to the association between CaM and eNOS. Citrulline formation and cytochrome c reduction assays revealed that in comparison with nNOS or iNOS, eNOS was less stringent in the requirement of calcium binding to each of four calcium-binding sites. However, lobe-specific disruption with double mutations in calcium-binding sites either at N- (B12Q) or at C-terminal (B34Q) lobes greatly diminished both eNOS oxygenase and reductase activities. Gel mobility shift assay and flavin fluorescence measurement indicated that N- and C-lobes of CaM played distinct roles in regulating eNOS catalysis; the C-terminal EF-hands in its calcium-bound form was responsible for the binding of canonical CaM-binding domain, while N-terminal EF-hands in its calcium-bound form controlled the movement of FMN domain. Limited proteolysis studies further demonstrated that B12Q and B34Q induced different conformational change in eNOS.

Conclusions: Our results clearly demonstrate that CaM controls eNOS electron transfer primarily through its lobe-specific calcium binding.

Citation: Wu P-R, Kuo C-C, Yet S-F, Liou J-Y, Wu KK, et al. (2012) Lobe-Specific Calcium Binding in Calmodulin Regulates Endothelial Nitric Oxide Synthase Activation. PLoS ONE 7(6): e39851. doi:10.1371/journal.pone.0039851

Editor: Andreas Hofmann, Griffith University, Australia

Received March 16, 2012; **Accepted** May 31, 2012; **Published** June 29, 2012

Funding: The work was supported by the Grant of National Health Research Institutes (99A1-CSAP01-014) at Taiwan. The funders had no role in study design, data collection and analysis, decision to publish, or preparation of the manuscript.

Competing Interests: The authors have declared that no competing interests exist.

* E-mail: 990419@nhri.org.tw (PFC); kkgo@nhri.org.tw (KKW)

Introduction

Human endothelial nitric oxide synthase (eNOS) catalyzes the synthesis of nitric oxide (•NO), which is a key regulator of cardiovascular homeostasis [1,2]. Like neuronal NOS (nNOS) [3,4] and macrophage inducible NOS (iNOS) [5,6], eNOS [7] is a homodimer; each monomer contains a C-terminal reductase domain, and an N-terminal oxygenase domain [8–10]. The reductase domain binds FAD and FMN cofactors, and consists of NADPH binding site, while the oxygenase domain binds protoporphrin IX heme, tetrahydrobiopterin (H_4B), and contains the site for L-arginine binding. These two domains are connected by a canonical CaM-binding sequence. Binding of calcium/CaM to this site facilitates intra-domain electron transfer between FAD and FMN as well as inter-domain electron transfer from the flavin of one subunit to the heme of the other subunit [11–13]. Although the mechanism by which CaM regulates NOS activation has been under intensive investigation, much remains unresolved. Our recent work on eNOS has demonstrated that in addition to the putative CaM binding domain (residues 491–510, hereafter referred to simply as CBD) [14], two other regions, *i.e.* residues 174–193 of the heme-binding site and residues 729–757 located at the hinge region connecting FAD and FMN subdomains, are possibly involved in CaM/calcium-regulated eNOS activation and deactivation [15]. Thus, the mechanisms underlying CaM/calcium-dependent eNOS catalysis are more complicated than previously thought.

CaM is a ubiquitous calcium-binding protein, structurally resembling a dumbbell. It contains N- and C-terminal lobes joined by a flexible helical linker [16]. Each lobe comprises two E–F hands with two calcium-binding sites. The calcium-binding sites in the C-terminal lobe (sites 3 and 4) have a higher affinity for calcium than those in the N-terminal lobe (sites 1 and 2) [17]. Calcium binding triggers conformational changes of CaM, bringing the two lobes together, forming a hydrophobic interface to interact with its target proteins [18].

CaM regulates all three NOS isoforms. iNOS binds CaM tightly at low calcium level and is catalytically active at basal cellular calcium concentrations [19], while eNOS and nNOS bind CaM reversibly in a calcium concentration-dependent manner and require high calcium concentrations for catalysis [7,20]. Previous reports using CaM mutants with different calcium-binding site mutations suggest differential roles of the four calcium-binding sites for nNOS and iNOS in regulating CaM binding and electron transfer [21–23]. The role that each calcium-binding site plays in regulating CaM binding to eNOS and eNOS catalytic activity is unclear. As eNOS is attached to plasma

membrane through myristoylation and palmitaylation, calcium-CaM dependent electron transfer and catalysis are likely to be influenced by diverse signaling pathways making it more complicated than iNOS or nNOS [24]. Furthermore, since the calcium-binding sites of CaM can differentially regulate target protein function, and a large fraction of free CaM is not fully occupied with four calcium ions in fluctuating intracellular calcium concentration [25], it is essential to clarify the role of each calcium-binding site of CaM in eNOS activity.

Electron flow in NOS isoforms is controlled by CaM/calcium binding. In the absence of CaM, the FMN domain is in a shielded state (input) which is locked by NADPH binding [26] and stabilized by the relative spatial arrangements of autoinhibitory elements and C-terminal tail. In this state, the FMN domain is in close contact with the FAD/NADPH binding domain [27], and electron transfer is limited to FAD to FMN and not to other electron acceptors. CaM/calcium binding elicits a swing of FMN domain toward a deshielded (output) state, which facilitates electron transfer to heme/H_4B or cytochrome c [28–31]. The N- and C-terminal lobes of CaM bind calcium ions with different affinities and lobe-specific functions of CaM are frequently seen in the regulation of its target proteins [32,33]. We hypothesized that the shift of FMN subdomain from input to output states for electron transfer depends on lobe-specific calcium/CaM binding to eNOS. To test this hypothesis, we mutated a single calcium-binding site (designated B_{1Q}, B_{2Q}, B_{3Q} and B_{4Q}, respectively), both binding sites at N-lobe (B_{12Q}) or C-lobe (B_{34Q}) or all four calcium-binding sites (B_{1234Q}), and assessed how these mutations impact CaM binding to CaM binding domain and CaM-mediated eNOS conformational change, and catalytic activities.

Table 1. The primers used for mutations and the residues changed for each mutant.

Mutants	Primers	Residue changed
B1Q	5′-CACCACCAAG**CAA**TTGGGGACAGTGAT-3′	E_{31}–Q_{31}
	5′-ATCACTGTCCCCAA**TTG**CTTGGTGGTG-3′	
B2Q	5′-CTTCCCG**CAG**TTCTTAACCATGATG-3′	E_{67}–Q_{67}
	5′-CATCATGGTTAAGAA**CTG**CGGGAAG-3	
B3Q	5′-CTACATCAGCGCTGCG**CAG**CTGCGT-3′	E_{104}–Q_{104}
	5′-ACGCAG**CTG**CGC AGCGCTGATGTAG-3′	
B4Q	5′-GGCCAGGTTAACTATGAA**CAG**TTTGTA-3′	E_{140}–Q_{140}
	5′-TACAAA**CTG**TTCATAGTTAACCTGGCC-3′	
B12Q		E_{31}–Q_{31}
		E_{67}–Q_{67}
B34Q		E_{104}–Q_{104}
		E_{140}–Q_{140}
B1234Q		E_{31}–Q_{31}
		E_{67}–Q_{67}
		E_{104}–Q_{104}
		E_{140}–Q_{140}

doi:10.1371/journal.pone.0039851.t001

Results

CaM mutants in eNOS activation

CaM mutants carrying various E to Q substitutions at calcium-binding sites were generated based on the sequence of human CaM shown in Figure 1A. Primers used to generate CaM mutants

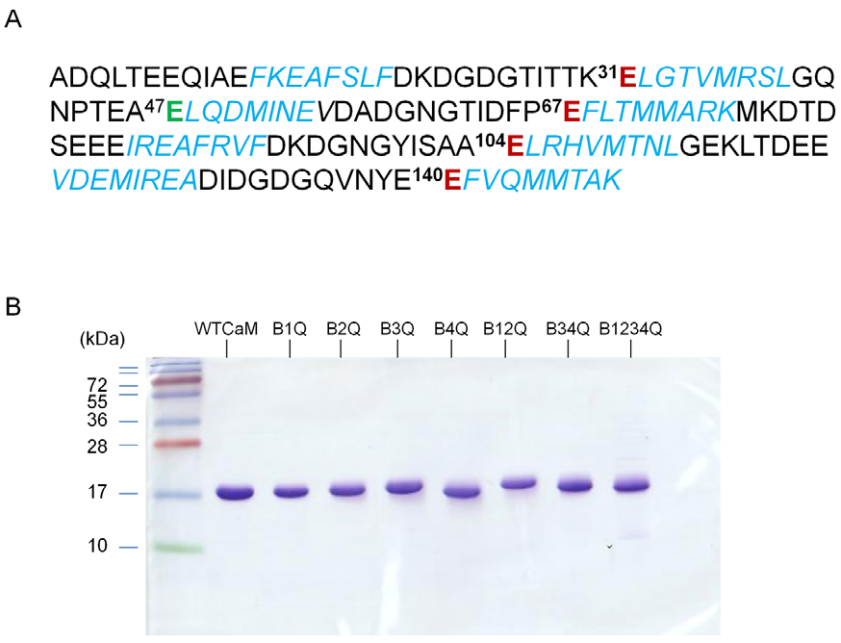

Figure 1. CaM mutant constructs. A: The sequence of human CaM is shown, using single-letter amino acid residue codes. The mutated amino acid residue in each calcium-binding site is marked in red. Helical regions are shown in Italics and blue color. B: The electrophoretic mobility of wild-type and mutant CaM proteins was analyzed by SDS-PAGE. A 5-μg sample of each CaM construct was loaded in a 15% SDS-PAGE which was run with a standard Laemmli SDS-PAGE buffer in the presence of 1 mM EGTA. Molecular masses of protein standards are shown on the left in kilodaltons (kDa).
doi:10.1371/journal.pone.0039851.g001

and the designated names for each mutant were listed in Table 1. Purified CaM mutants were at least 95% pure with an estimated molecular mass of ~17 kDa based on SDS-PAGE analysis, which was run in a standard SDS-PAGE buffer containing 1 mM EGTA. We generally obtained about 16 to 100 mg purified proteins from a liter of culture medium. The electrophoretic mobility of most mutants was not obviously different from that of the wild-type CaM, with the exception of B_{4Q} mutant which had slightly higher mobility (Figure 1B).

The steady-state citrulline formation was used to determine electron flux from NADPH to the heme of oxygenase domain. Effects of wild-type and mutant CaMs on citrulline formation was evaluated by adding increasing concentrations of CaM to the assay mixture. Concentration response curves for wild-type CaM and each mutant are shown in Figure 2. Compared to wild-type CaM, B_{1234Q} showed no activation at all while B_{12Q} and B_{34Q} greatly diminished ability to activate citrulline formation through their wide-ranging concentrations. The response curves of the four single-site mutants (B_{1Q}, B_{2Q}, B_{3Q}, and B_{4Q}) resembled the wild-type response curve. Quantitative analysis from multiple experiments revealed that the EC_{50} (concentration required for half maximal citrulline formation) for the single-site mutants is about 2–3 fold higher than that of wild-type (Table 2). These data suggest that each of the four calcium-binding sites supports the association between CaM and eNOS (Table 2).

As CaM concentrations increased, some mutants exhibited citrulline forming activity even higher than wild-type CaM. We compared the citrulline formation in the presence of saturating concentrations for each CaM construct (0.5 μM), and activity obtained with eNOS bound to wild-type CaM was set to 100%. As shown in Figure 3A, the wild-type CaM increased citrulline formation ~50-fold above that observed in the absence of CaM. Maximal citrulline formation with B_{1Q} was reduced by 25% and B_{2Q} was not significantly different from the wild-type (Figure 3A), while maximal citrulline formation of B_{3Q} and B_{4Q} was slightly higher than that of the wild-type. Of the two double mutants, the extent of maximal activity with B_{12Q} and B_{34Q} was reduced to 24% and 18% of the wild-type, respectively. The activity with

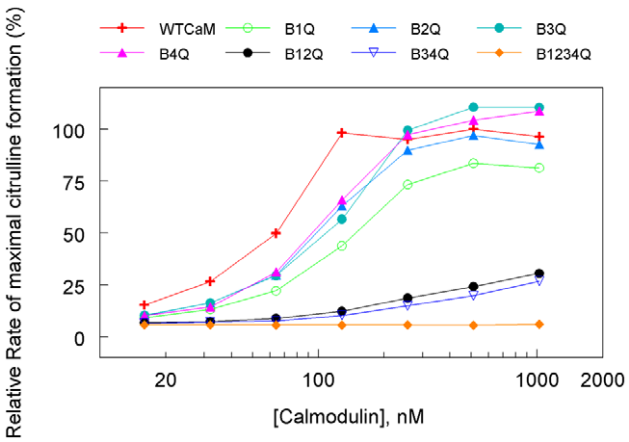

Figure 2. Citrulline formation as a function of CaM concentrations. Citrulline forming activity was determined in a reaction mixture containing 25 mM Tris, pH 7.5, 100 nM eNOS, 3H-L-arginine (**1**μCi), L-arginine (20 μM), NADPH (100μM), H_4B (10μM), and $CaCl_2$ (300 μM), 0.2 mM EDTA, 100 mM NaCl, 0.1 mM DTT, 10% glycerol and the indicated concentration of each CaM construct as described under Experimental Procedures. Data are mean of duplicate measurements with <5% variation. Each experiment was repeated three times.
doi:10.1371/journal.pone.0039851.g002

Table 2. The EC_{50} for each CaM construct in activation of eNOS citrulline formation.

Mutants	EC_{50} (nM)
WTCaM	75±10
B1Q	161±14
B2Q	125±12
B3Q	170±16
B4Q	148±8

The *bar values* represent the means ± standard deviation. The mean values were obtained from three independently prepared batches of proteins.
doi:10.1371/journal.pone.0039851.t002

B_{1234Q} was not increased and remained at the level without CaM (Figure 3A). The result indicates that except for B_{1Q}, single mutation at calcium-binding site of CaM has little effect on eNOS citrulline forming activity while disruption in two calcium-binding sites either at N- (B_{12Q}) or at C-terminal (B_{34Q}) lobe greatly impacts eNOS oxygenase activity.

We next evaluated the effect of CaM mutants on eNOS reductase activity. *Cytochrome c* accepts electrons exclusively from the FMN domain and has been used to measure electron flow within the reductase domain. Binding of wild-type CaM to eNOS induced a ~4-fold increase in *cytochrome c* reduction. B_{3Q} mutant increased *cytochrome c* reduction to a level comparable to wild-type CaM (Figure 3B). On the other hand, *cytochrome c* reduction induced by B_{1Q}, B_{2Q} and B_{4Q} was 63%, 67% and 55% of the wild-type level, respectively. The multiple mutants, *i.e.* B_{12Q}, B_{34Q} and B_{1234Q} exhibited slight or no increase in *cytochrome c* reductase activity. These results demonstrate that with the exception of B_{3Q}, single mutation at calcium-binding sites in CaM affects the reductase activity greater than the oxygenase activity in eNOS. Furthermore, full calcium bindings at N- and C-terminal lobes are essential for electron transfer through the eNOS reductase domain (Figure 3B).

Binding of CaM mutants to eNOS CaM binding domain (CBD) Peptide

The ability of various CaM mutants to bind CBD was evaluated. Each CaM mutant was incubated with CBD in the presence of 100 μM calcium at several different peptide:CaM ratios. The CBD-CaM complexes and free CaM were examined by nonreducing, nondenaturing electrophoresis. Free peptides were not detected because they are positively charged at neutral pH and therefore will have an upward mobility toward cathode and do not enter the gel [34,35]. In the presence of EGTA, no mobility shift bands were detected for wild-type or any CaM mutant (data not shown). Peptide-CaM complexes can be seen above free CaM band in the presence of 100 μM calcium. The extent of CaM-peptide interaction is assessed by measuring attenuation of free CaM bands and the shift in the mobility of the CaM protein with increasing peptide concentration. As shown in Figure 4, B_{1Q}, B_{2Q} and B_{3Q} bound CBD with an affinity similar to the wild-type CaM. B_{4Q} and B_{12Q} bound CBD but the binding was not complete. B_{34Q} and B_{1234Q} did not bind CBD. These results suggest that the canonical CaM-binding site on eNOS interacts with the calcium-bound C-lobe in CaM.

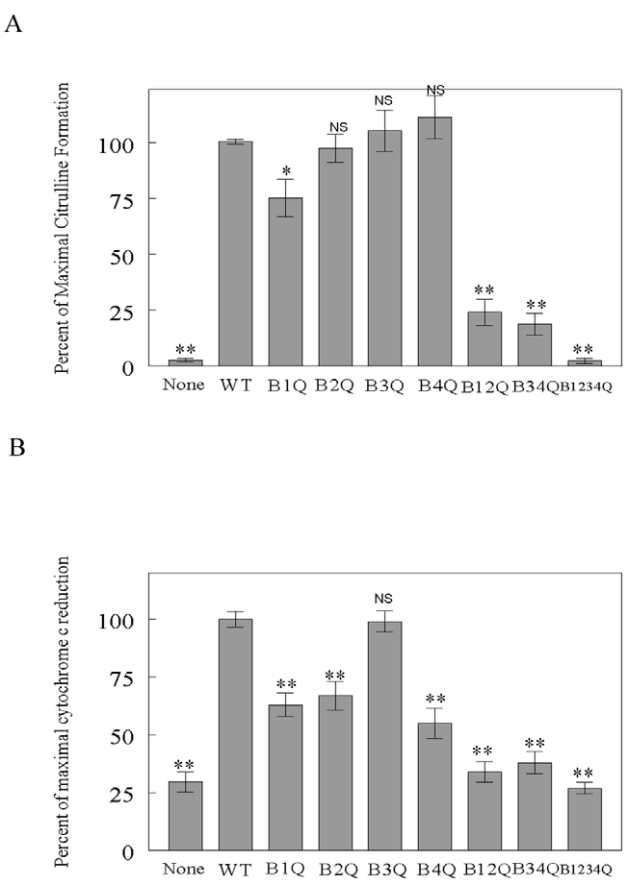

Figure 3. Ability of various CaM mutants to activate eNOS enzymes. A: Citrulline formation activity. B: *Cytochrome c* reduction activity. Both citrulline formation and *cytochrome c* reduction were measured in the presence of saturating concentration of each CaM construct (0.5 μM). NOS activities were expressed as percentage of the respective maximal NOS activity (100%) which was obtained with the eNOS bound to wild-type CaM. Under these conditions, the activities for eNOS bound to wild-type CaM were ~14 min^{-1} for citrulline formation, and ~286 min^{-1} for *cytochrome c* reduction. Data are presented as means±standard deviation. * denotes $p<0.05$, ** <0.01, NS, not significant difference as compared to wild-type CaM. Each experiment was performed in triplicate and repeated three times.
doi:10.1371/journal.pone.0039851.g003

Distinct roles of CaM N- and C-Terminal lobes on eNOS Flavin Fluorescence

Since the N- and C-terminal lobes of CaM can function as an independent domain [33,36], we determined whether a conversion of the FMN subdomain from shielded to deshielded state depends on calcium-bound N- and C-terminal lobes of CaM. As the intensity of flavin fluorescence is proportional to the degree of FMN deshielding [37], we monitored the change in flavin fluorescence of eNOS induced by wild-type CaM, B_{12Q} or B_{34Q} in the presence or absence of calcium. As shown in Figure 5A, wild-type and mutant CaMs were unable to increase flavin fluorescence of eNOS in the presence of 2 mM EGTA. Upon addition of calcium, B_{34Q} increased flavin fluorescence intensity to the same level as the wild-type CaM. In contrast, B_{12Q} increased much less fluorescence intensity compared with wild-type CaM or B_{34Q}, indicating that the N-terminal EF-hands in its calcium-bound form are responsible for the input/output swing of FMN domain (Figure 5B).

Trypsinolysis of eNOS in the presence of wild-type CaM, B12Q or B34Q

As the results shown above have provided evidence that CaM N- and C-terminal lobes in its calcium-bound form play distinct roles in interacting with CaM binding domain and in the shift of input/output state of FMN domain, we speculated that binding of these two lobes might induce different conformational changes in eNOS. We used limited trypsin digestion to detect the eNOS conformation changes induced by wild-type vs. B_{12Q} or B_{34Q}. Limited trypsinolysis of eNOS was carried out in the presence of high or low calcium concentrations.

In the absence of calcium, trypsinolysis of eNOS incubated with wild-type, B_{12Q} or B_{34Q} produced an identical fragment profile with one major band having apparent molecular mass of ~ 56 kDa. N-terminal sequencing revealed that this band was composed of two portions of N-terminal sequences of K^{29}QGPA (fragment-1a in Figure 6A) and K^{498}EVAN (fragment-2a in Figure 6A), indicating two cleavage sites: (1) between Lys28 and Gln29 and (2) between Lys497 and Glu498. Lys28 is close to the palmitoylation site, and Lys497 is within the canonical CaM-binding domain of eNOS (Figure 6C), reflecting that without CaM protection, CaM-binding domain of eNOS is sensitive to trypsin digestion.

In the presence of calcium, trypsin digestion of eNOS with wild-type CaM yielded three notable bands ~67 kDa (fragment-1b), ~58 kDa (fragment-2b) and ~52 kDa(fragment-4b & 5b) (Figure 6B). N-terminal sequencing of ~67 kDa band revealed the cleavage site at K^{29}QGPA and judged from the apparent size, the C-terminal tryptic site is probably around Arg630 which is situated in the autoinhibitory (AI) region (Figure 6C, fragment-1b), consistent with the previous report that calcium/CaM binding induces eNOS conformational change resulting in the exposure of the autoinhibitory elements [38]. N-terminal sequencing of the ~58-kDa band showed the cleavage site at K^{29}QGPA and C-terminal tryptic residue at approximately 549, based on size estimate (fragment-2b in Figure 6C). N-terminal sequencing of ~52 kDa band revealed two N-terminal sequences: (1) fragment-4b with N-terminal sequence of R^{722}DIFS and an estimated C-terminal end at residue 1203, and (2) fragment-5b with N-terminal sequence of K^{517}RVKA and an estimated C-terminal end at residue 994 (Figure 6C).

Trypsin digestion of eNOS with B_{12Q} produced a similar fragment profile as that with wild-type CaM, except that a portion of N-terminal sequence of fragment-3b was not detected in wild-type CaM and fragment 5b was not detected in B_{12Q} (Figure 6B). The N-terminal sequence of fragment-3b is K^{498}EVAN that is within canonical CaM-binding domain at eNOS (Figure 6C). By contrast, the fragment profile of eNOS trypsinolysis with B_{34Q} revealed an attenuated fragment-1b and enhanced fragment-2b and 3b as well as fragments 4b and 5b. The trypsinolysis data provide important insights into the influence of CaM on eNOS conformation: (1) Cleavage of eNOS at Lys28 was observed either in the presence or absence of CaM, indicating that the sequence at this residue near the palmitoylation site is in an exposed area. The eNOS is dually acylated by *N*-myristoylation at Gly2 and by thiopalmitoylations at Cys15 and Cys26 [39,40]. As palmitoylation is reversible, whether existence of regulated cycles of palmitoylation and depalmitoylation controls eNOS degradation remains further investigation; (2) N-terminal sequence of K^{498}EVAN (fragment-3b) was detected with B_{12Q} and B_{34Q} but not with wild-type CaM; the intensity of fragment-3b in B_{12Q} was weaker than in B_{34Q}. This is consistent with the gel mobility shift assay, in which B_{12Q} binds CaM binding domain but not as well as wild-type CaM; B_{34Q} shows no binding at all. The result further confirms that C-terminal lobe in its calcium-bound form can

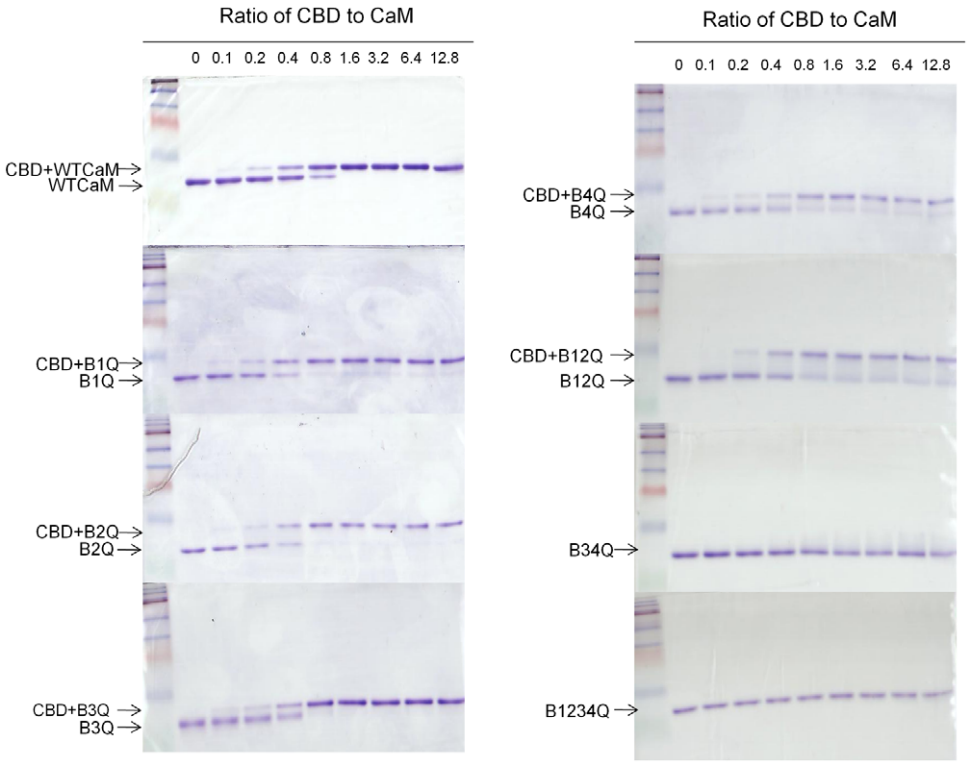

Figure 4. Interaction of CaM-binding domain with each CaM construct. The canonical CaM-binding domain of human eNOS (CBD, residues 491–510) was incubated with CaM constructs (200 pmol) by increasing peptide:CaM molar ratios at room temperature for 1 h before electrophoresis in the presence of 100 μM of calcium. The samples were analyzed on 18% non-denaturing gels and visualized with Coomassie Blue R-250. The first lane in each gel contains CaM only, *i.e.* CBD/CaM ratio is 0. The rest CBD/CaM ratios were indicated. CBD-CaM complexes and free CaM are denoted.
doi:10.1371/journal.pone.0039851.g004

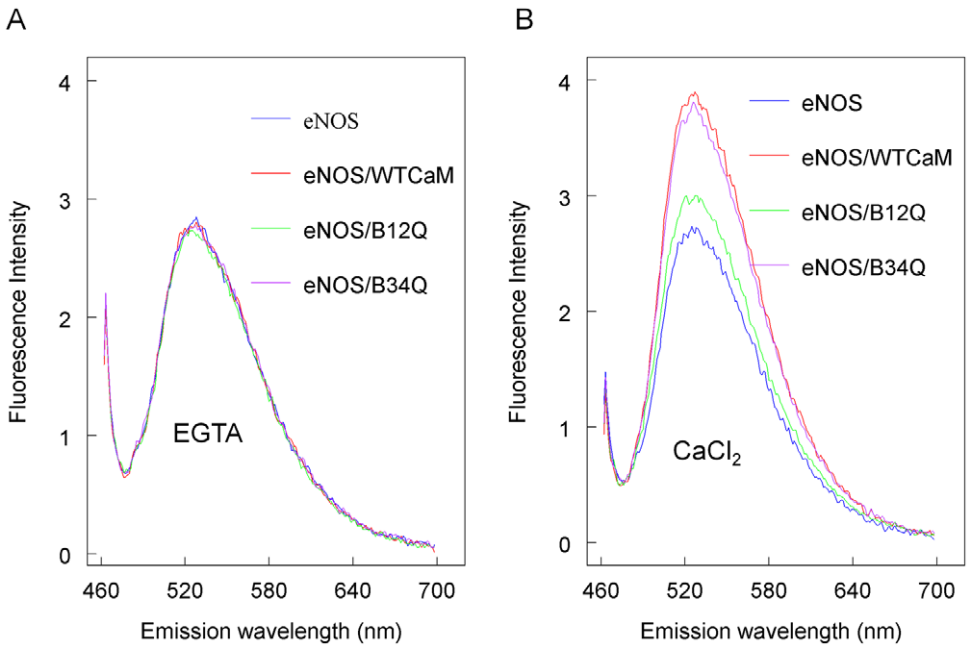

Figure 5. Flavin fluorescence of eNOS treated with wild-type and CaM mutants. A: Fluorescence emission spectra of eNOS were obtained in a solution containing 25 mM Tris, pH 7.5, 100 mM NaCl, 0.1 mM DTT, ~6 μM eNOS and ~12μM of wild-type CaM, B_{12Q} or B_{34Q} in the presence of 2 mM EGTA. B: The change of fluorescence intensity for wild-type CaM, B_{12Q} or B_{34Q} was recorded upon addition of 2.5 mM $CaCl_2$ to the above mixtures. Excitation wavelength was set at 455 nm. The fluorescence data were corrected by subtracting CaM and buffer effects. The eNOS alone and eNOS-CaM complex are indicated in each plot.
doi:10.1371/journal.pone.0039851.g005

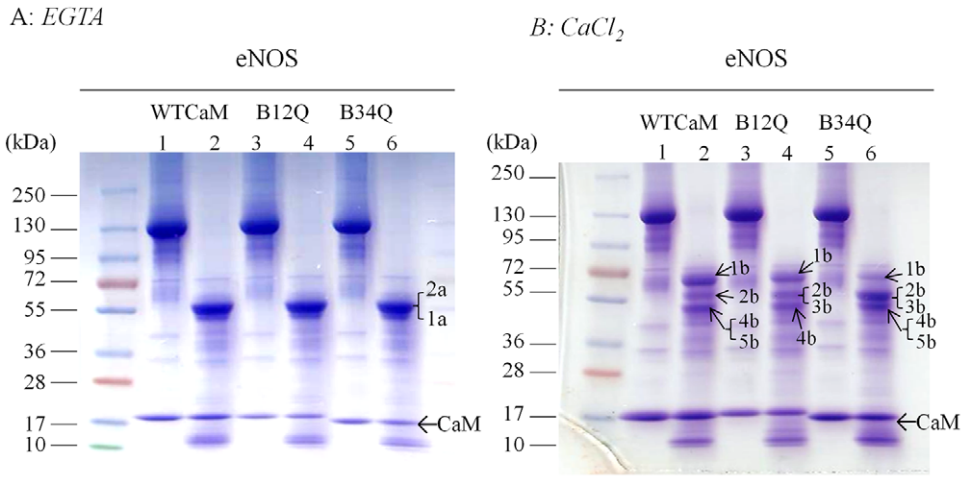

C: Relative Position of tryptic fragments in eNOS

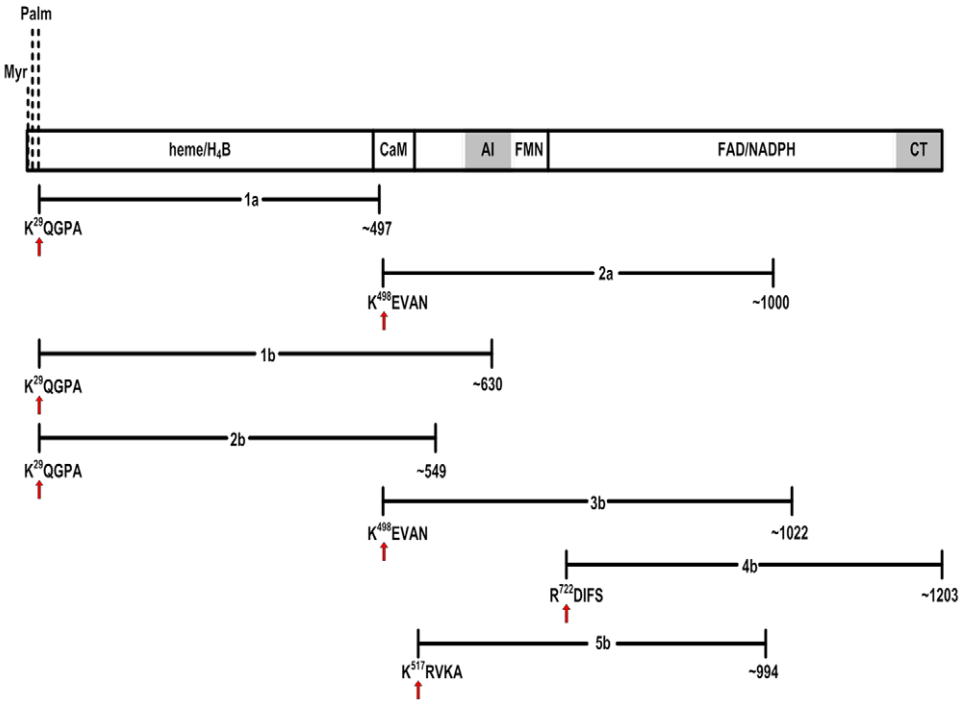

Figure 6. Limited trypsinolysis of eNOS in the presence of wild-type CaM, B_{12Q} or B_{34Q}. A: Trypsinolysis of eNOS (~5μM) was performed in the presence of 10 μM of wild-type CaM, B_{12Q} or B_{34Q} at 22°C for 15 min with 1 mM EGTA. B: Trypsinolysis was carried out in the presence of 100 μM $CaCl_2$. Lane 1: undigested eNOS with wild-type CaM; lane 2: trypsinized eNOS with wild-type CaM; lane 3: undigested eNOS with B_{12Q}; lane 4: trypsinized eNOS with B_{12Q}; lane 5: undigested eNOS with B_{34Q}; lane 6: trypsinized eNOS with B_{34Q}. Molecular masses of marker proteins are shown on the *left* in kilodaltons (kDa). Following SDS-PAGE, the tryptic samples were transferred to PVDF membranes using CAPS buffer for 3 h at 50 V and 4°C. The bands excised for N-terminal sequencing are indicated. C: Relative position of N-terminal sequences of the indicated tryptic fragments in the schematic eNOS structure. The C-terminal termination sites are unknown and the residue at C-terminal end in each tryptic fragment was approximately estimated from the apparent molecular mass. Red arrow depicts the tryptic cleavage site. The blocks indicate binding sites for heme, H_4B, CaM, FMN, FAD and NADPH. AI and CT refer to autoinhibitory loop and C-terminal tail, respectively. The myristoylation site (Myr.) and palmitoylation sites (Palm.) are denoted.
doi:10.1371/journal.pone.0039851.g006

protect eNOS CaM binding domain from tryptic digest; (3) binding of eNOS by wild-type, B_{12Q} or B_{34Q} similarly resulted in the exposure of R^{722}DIFS to trypsin digestion. This sequence is situated at the hinge region between FMN and FAD domains (Figure 6C). Our previous finding has suggested that this region may interact with CaM and is involved in eNOS catalysis [15]. That binding of wild-type or CaM mutants impaired in calcium-binding at C- or N-lobe caused a similar exposure of the hinge region, suggests highly flexible nature of this region, which is likely to serve as a pivot for the motion of FMN domain [41]; (4)

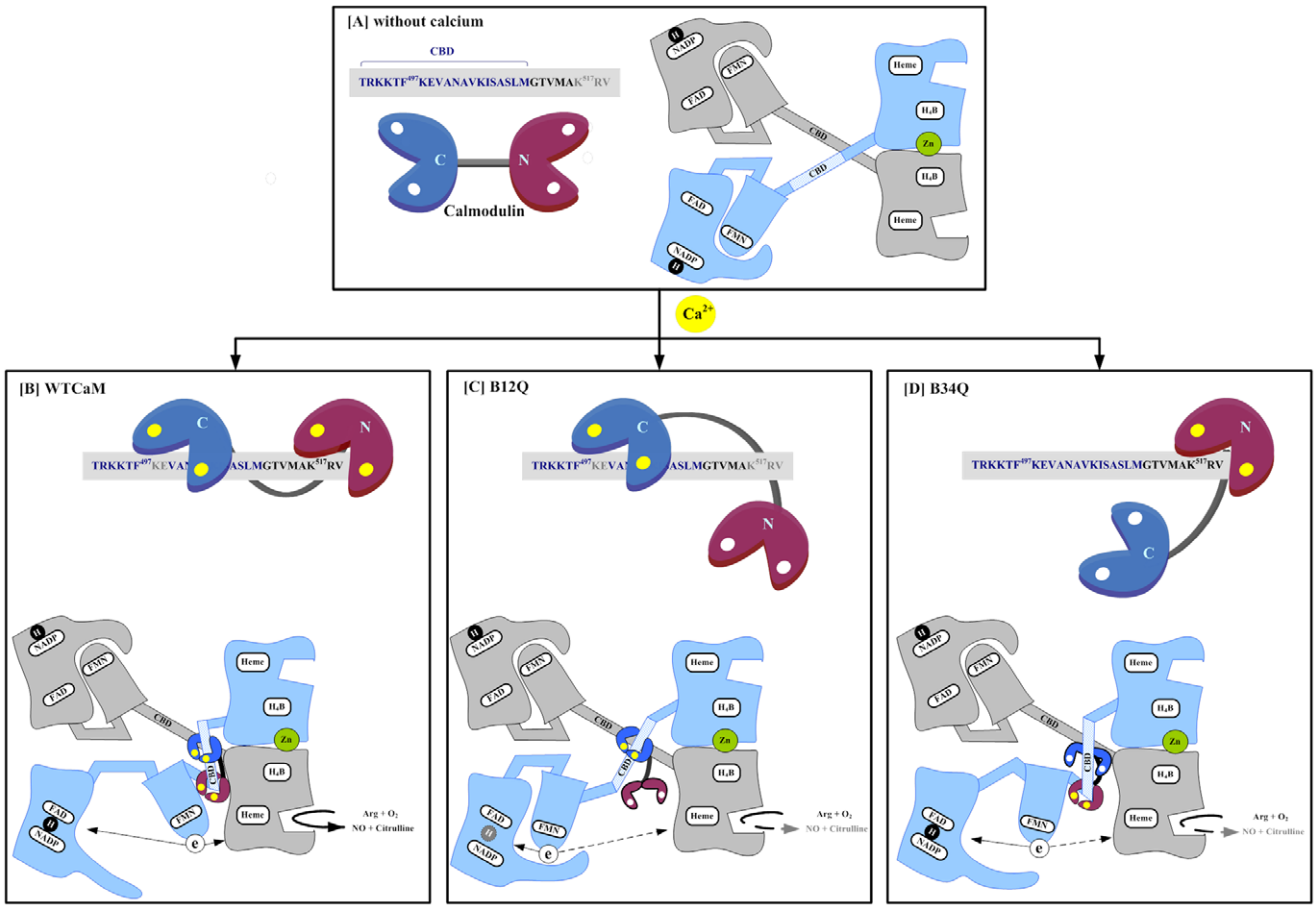

Figure 7. Schematic illustration of differential regulation of eNOS electron transfer by N- and C-terminal lobes of CaM. Dimeric eNOS model is derived from Daff [44]. The *gray colored* domains represent one subunit, and the *sky-blue colored* domains represent the other. The blocks indicate binding sites for heme, H_4B, zinc, CaM, FMN, FAD and NADPH. The canonical CaM-binding domain (residues 491–510) between the FMN domain and the heme domain is denoted as CBD. CaM shown as two *lobed structures* N and C, joined by a flexible linker is adapted from Ref 45; apoCaM is marked with white circles and calcium binding is indicated by yellow circles. A: In the absence of calcium, apo-CaM is not associated with eNOS in which Lys497 is exposed to the trypsin digestion; the FMN domain is locked with FAD domain and electron flux is blocked. B: Upon calcium binding, wild-type CaM wraps around the eNOS CBD and potentially other sites with its two lobes bound. This binding protects Lys497 from tryptic cleavage and exposes Arg517 for trypsinolysis. Consequently, the FMN domain is released from the FAD domain, becoming accessible to the heme domain of the opposite subunit. C: With B_{12Q} mutation of N-lobe, calcium-bound C-lobe binds normally to CBD while the mutated N-lobe could not bind calcium and is unable to bring FMN domain to the heme domain of the other subunit which hinders electron transfer as illustrated by a dotted line. D: With B_{34Q} mutation of C-lobe, C-lobe is unable to bind CBD which retards electron transfer.
doi:10.1371/journal.pone.0039851.g007

Exposure of K^{517}RVKA (fragment-5b) with wild-type and B_{34Q} binding but not B_{12Q} binding suggests that binding of CaM N-terminal lobe in calcium-bound form exposes Arg517 for trypsin digestion. eNOS Arg517 is analogous to iNOS Arg536 and nNOS Arg757 which are reported to form both salt bridge and hydrogen bonding interaction with CaM Glu47 and several backbone oxygens in NOS FMN subdomain [42], and are considered to be crucial for control of FMN subdomain interactions with its redox partners [43].

Discussion

The results indicate that each calcium-binding site on CaM plays a part in mediating CaM-induced eNOS electron transfer and catalytic activity. Single mutation of each binding site results in an increased EC50 by ~2–3 fold over the wild-type without a substantial effect on maximal citrulline formation. However, double mutation of binding sites at the C-lobe or N-lobe of CaM drastically reduces maximal citrulline formation and *cytochrome c* reduction, indicating requirements of lobe-specific calcium binding for eNOS reductase and oxygenase activities. Gel mobility shift assay, flavin fluorescence measurements and limited trypsinolysis demonstrate that the N- and C-terminal lobes play a distinct role in eNOS activation, *i.e.* N-lobe in its calcium-bound form controls FMN subdomain motion, while C-lobe in its calcium-bound form binds CaM binding domain region in eNOS.

Taken together the results from our current study, we outlined these findings in a schematic diagram based upon NOS dimeric model from Daff [44] and CaM bi-lobed structure from Rodney *et al.* [45], illustrating how N- and C-terminal lobes of CaM differentially regulate eNOS catalysis (Figure 7). In the absence of calcium, apo-CaM is not associated with eNOS in which Lys497 is sensitive to trypsin digestion; the FMN domain, closely associated with FAD domain, is in the locked position and electron flux is blocked (Figure 7A). Upon calcium binding, wild-type CaM undergoes a conformational change; wraps around the CaM-binding domain and potentially other CaM-binding sites in eNOS with its two lobes bound, as has been proposed for the multiple

CaM-binding sequences in the eNOS (15). The binding protects Lys497 from tryptic cleavage and exposes Arg517 for trypsinolysis. Consequently, the FMN domain is released from the closed to the open position, becoming accessible to the heme domain of the opposite subunit or to an exogenous electron acceptor like *cytochrome c* (Figure 7B). With B_{12Q} double mutation of N-lobe, CaM is tethered to the N-terminus of eNOS CaM-binding domain solely by calcium- bound C-lobe. This association protects Lys497 from tryptic cleavage with slight induction of the FMN domain mobility. In this state, the FMN domain is mainly in the locked position, resulting in great attenuation of eNOS activity. (Figure 7C). With B_{34Q} double mutation of C-lobe, calcium-bound N-lobe is unable to protect Lys497 from tryptic cleavage but exposes Arg517 for trypsinolysis and increases flavin fluorescence to the same level as wild-type CaM. This implies that B_{34Q} does not bind to CaM-binding domain but rather to a region adjacent to CaM-binding domain. In this state, although the FMN domain is in the open position, both eNOS oxygenase and reductase activities are greatly attenuated, indicating that the released FMN domain no longer associates with its redox partners as it normally would (Figure 7D). This clearly shows that binding between CaM and CaM-binding domain of eNOS is head-to-tail with the C-lobe of CaM bound to the N-portion of CaM-binding domain. Lobe-specific calcium binding is crucial for CaM to control eNOS electron transfer, and efficient activation requires both CaM N- and C-terminal lobes in its calcium-bound form to interact with CaM-binding domain as well as with other CaM-binding elements in eNOS.

Comparison of the calcium-binding site mutations on citrulline formation and *cytochrome c* reduction in eNOS vs. the other isoforms reveal significant differences. As shown in Table 3, single calcium-binding site mutation of CaM exerts effect on eNOS activation less than on nNOS or iNOS. Notably, B_{1Q} mutant reduced eNOS citrulline formation by 25% but completely abolished nNOS citrulline formation [21] and conversely did not influence iNOS citrulline formation [22]. On the other hand, B_{3Q} mutant which did not affect eNOS and caused a mild reduction of nNOS citrulline formation reduced iNOS citrulline formation by >50% while B_{4Q} which increased eNOS citrulline formation caused a profound reduction of nNOS but had little effect on iNOS citrulline formation. B_{2Q} did not significantly influence eNOS citrulline formation but exerted a great effect on nNOS and iNOS citrulline formation. B_{3Q} selectively reduced iNOS citrulline formation whereas B_{4Q} reduced nNOS citrulline formation. The effect of a single site mutation on *cytochrome c* reduction is concordant with that on citrulline formation with the exception of B_{4Q} which reduces cytocrome c reduction without a significant effect on citrulline formation. Our data reveal that lobe-specific mutation of calcium-binding sites (B_{12Q} and B_{34Q} alike) severely interferes with eNOS and nNOS activity without an effect on iNOS (23). These results provide evidence for differential effects of CaM calcium-binding status on electron flow and catalytic activity in eNOS vs. nNOS and iNOS.

B_{4Q} in comparison with wild-type CaM attenuated *cytochrome c* reduction by ~45% while it increased citrulline formation (Figure 3B vs. 3A). This differential effect is unexpected as the crystallographic analysis of CaM bound to eNOS CaM-binding domain [14] or nNOS CaM-binding domain as well as CaM-iNOS FMN subdomain complex [42] has shown interaction of CaM with the canonical CaM-binding site of all three NOS isoforms in an anti-parallel orientation in which the B_{4Q} site (E140 of CaM) interacts with the N-terminal portion of CaM-binding domain situated in the vicinity NOS oxygenase domain. It is unclear how mutation of this site only affects reductase activity without reducing oxygenase activity. The results nevertheless support the notion that CaM activates reductase and oxygenase by distinct mechanisms [46].

Table 3. Differential effect of mutating Ca^{2+}-binding sites at CaM on enzyme activation among NOS isoforms.

	Cyto c Reduction			Citrulline formation or NO production		
	eNOS	nNOS	iNOS	eNOS	nNOS	iNOS
CaMs	(%)			(%)		
None	30±4[a]	4.2 [b]		2.8±0.8 [a]	0.47 [b]	
WT	100±12 [a]	100[b]	100[c]	100±2[a]	100[b]	100[c]
B_{1Q}	63±7 [a]	11[b]	109[c]	75±4[a]	<2[b]	95[c]
B_{2Q}	67±6 [a]	~50[b]	64[c]	94±6[a]	26[b]	41[c]
B_{3Q}	99±11 [a]	76[b]	67.7[c]	105±9[a]	82[b]	43[c]
B_{4Q}	55±7 [a]	~53[b]	42.8[c]	111±13 [a]	30[b]	90[c]
B_{12Q}	34±4 [a]	~6[d]	140[d]	24±6[a]	~5[d]	75[d]
B_{34Q}	38±5 [a]	~12[d]	100[d]	18±5[a]	~10[d]	115[d]
B_{1234Q}	27±3 [a]	~11[d]	<25[d]	2.3±0.4 [a]	<2[d]	<25[d]

[a]This manuscript: The activity was obtained in the presence of 0.5 μM CaM concentration. Under these conditions, the activities for eNOS bound to wild-type CaM were ~14 min^{-1} min^{-1} for citrulline formation, and ~286 min^{-1} for *cytochrome c* reduction.
[b]Data from Ref. 21.
[c]Data from Ref. 22.
[d]Data from Ref. 23.
doi:10.1371/journal.pone.0039851.t003

A recent crystal structure of a CaM-bound iNOS FMN subdomain [42] has shown that Glu47 located at the CaM N-terminal lobe participates in a bridging interaction with the iNOS FMN domain that helps transduce the effects of bound CaM. The authors suggested that an analogous CaM-FMN subdomain bridging interaction be expected to be present in the nNOS and eNOS enzymes. Tejero *et al.* later proved that this bridging connection appeared to control nNOS FMN subdomain movement [43]. Here, we propose that this bridging interaction is primarily controlled by lobe-specific calcium binding in CaM. Our flavin fluorescence data demonstrate that B_{34Q} is able to induce eNOS fluorescence intensity to the same level as the wild-type CaM, suggesting an interaction between CaM Glu47 and eNOS FMN subdomain which is present in an output state. However, B_{34Q} hardly increases eNOS oxygenase and reductase activities, possibly due to defective binding to CaM-binding domain. These data imply that attachment of calcium-bound C-terminal lobe of CaM to eNOS CaM-binding domain triggers FMN domain to be in a more suitable orientation for interacting with its redox partners. As B_{12Q} induced a much smaller increase in flavin fluorescence than wild-type CaM, it is possible that the bridging interaction between CaM Glu47 and eNOS FMN subdomain requires CaM N-terminal lobe in its calcium-bound form. From these findings, we conclude that calcium-bound C-lobe and N-lobe of CaM interact with eNOS at different regions in a coordinated manner that is necessary for the efficient electron transfer among different redox centers in eNOS.

Materials and Methods

Materials

L-[2,3,4,5^{-3}H] arginine (NET1123250UC) was obtained from PerkinElmer Inc. (6R)-5,6,7,8,-Tetrahydro-L-biopterin (H_4B) was

purchased from Research Biochemical International. Bradford protein dye reagent and electrophoretic chemicals were products of Bio-Rad. Restriction enzymes were from New Englands Biolabs. CaM-agarose, AG 50W-X8 (cation-exchange resin), NADPH and other reagents were obtained from Sigma. Sf21 insect cell was obtained from Clontech (ordering number 631411).

Mutagenesis

The human CaM cDNA was generously provided by Dr. Emanuel E Strehler. A series of single-point mutants of human CaM with Glu (E) to Gln (Q) substitutions at the *z* positions for coordinating calcium in each EF-hand, were generated by site-directed mutagenesis and termed as B_{1Q} (E31Q), B_{2Q} (E67Q), B_{3Q} (E104Q) and B_{4Q} (E140Q), respectively. Multiple point mutants unable to bind calcium either at the N-terminal lobe (B_{12Q}; E31Q and E67Q mutations), the C-terminal lobe (B_{34Q}; E104Q and E140Q mutations) or both lobes (B_{1234Q}; E31Q, E67Q, E104Q and E140Q) were subsequently prepared. The basic strategy for PCR-based mutagenesis was described previously [47]. The primers used for mutation and the residues changed for each mutant are listed in Table 1. The mutated residues glutamine (CAA or CAG) are highlighted with boldface. All primers were synthesized by MdBio Inc. (Taipei, Taiwan). Wild-type and mutant CaMs were cloned into pT7-7 vector through the NdeI and HindIII sites. The correct mutations were confirmed by Sequencing Service in the core facility of NHRI at Miaoli, Taiwan. The sequenced CaM genes were same as Genbank under accession number J04046.

Expression and Purification of Wild-type and Mutant CaMs

BL21 (DE3) transformed with each CaM construct were grown at 37°C in LB medium supplemented with 100 μg/ml ampicillin. The cultures were induced by 0.3 mM isopropy-β-D-thiogalacto-pyranoside when the OD_{600} reached to 0.8– 1.2 and harvested after overnight expression at room temperature. Purification of various CaMs was carried out essentially as described previously [15,48]. The CaM concentration was determined either by Bradford method [49] or spectrophotometry using $\epsilon_{277\ nm} = 2560\ M^{-1}\ cm^{-1}$.

Expression and Purification of eNOS

Human eNOS cDNA were inserted into *Eco*RI site of pVL1392 transfer vector, which was used to generate recombinant viruses in Sf21/baculovirus system. Due to low heme biosynthetic capability of Sf21 cells, supplemental heme chloride (4μg/ml) was added into the culture medium 18 h postinfection to enrich heme content of the expressed eNOS. Cells were harvested 60 h postinfection, suspended in buffer containing 25 mM Tris-HCl, pH 7.5, 0.2 mM dithiothreitol (DTT), 0.1 mM EDTA, 0.1 mM EGTA, 1 μM pepstatin A, 1μM leupeptin, 1 μM antipain, 1 μM phenylmethylsulfonyl fluoride, and 10% glycerol, and then sonicated 20 s for three times, centrifuged twice at 30,000×*g* for 20 min at 4°C. The supernatant was loaded onto a 2′, 5′-ADP-Sepharose affinity column (1.5×5 cm), proteins were eluted with a buffer containing 25 mM Tris-HCl, pH 7.5, 0.1 mM DTT, 20 mM 2′&3′-AMP mixture, 0.5 M NaCl and 10% glycerol. The eluate was diluted with 4-volume buffer containing 25 mM Tris-HCl, pH 7.5, 0.1 mM DTT, 100 μM $CaCl_2$ and 10% glycerol, and applied to a CaM-agarose column(1.5×5 cm) pre-equilibrated with buffer containing 25 mM Tris-HCl, pH 7.5, 0.1 mM DTT, 100 μM $CaCl_2$, 100 mM NaCl and 10% glycerol (Buffer A). The column was washed with Buffer A and eluted with buffer containing 25 mM Tris-HCl, pH 7.5, 0.1 mM DTT, 2 mM EGTA, 0.5M NaCl and 10% glycerol. The eluate was concentrated by Centriprep-50 (Millipore) and dialyzed against buffer containing 25 mM Tris-HCl, pH 7.5, 0.1 mM DTT, 100 mM NaCl and 10% glycerol.

Steady-state eNOS Activity

eNOS activity was determined by measuring conversion of L-[3H] arginine to L-[3H] citrulline as previously described [4] with slight modifications. The reaction mixture containing 25 mM Tris-HCl, pH 7.5, 0.1 mM DTT, 100 nM eNOS, 300 μM $CaCl_2$, 0.2 mM EDTA, 100 μM β-NADPH, 10 μM H_4B, 20 μM L-arginine, 10% glycerol, and 1μCi of L-[^{3}H] arginine was incubated at 37°C for 4 min either with a fixed amount (0.5 μM) or various concentrations of each CaM construct. *Cytochrome c* reduction was determined at room temperature in a reaction mixture containing 25 mM Tris-HCl, pH 7.5, 100 mM NaCl, 10% glycerol, 50 μM *cytochrome c*, 0.5 μM CaM, 100 μM $CaCl_2$, and 100 μM β-NADPH. The reaction was initiated by addition of 50 nM eNOS and monitored at 550 nm in a GE geneQuant100 spectrophotometer. Activity was determined using a ϵred-oxi of 21 $mM^{-1}cm^{-1}$.

Gel mobility-shift assay

A canonical CaM-binding peptide (CBD), TRKKTFKEVA-NAVKISASLM (eNOS residues 491–510) was synthesized by Peptide 2, Inc. (Chantilly, VA). Each CaM construct (200 pmol) was incubated with CBD at increasing molar ratios for 1 h at room temperature in a buffer (10 μl) containing 20 mM Tris, pH 7.5 with either 100 μM $CaCl_2$ or 1mM EGTA. The sample was subjected to 18% nondenaturing, non-reducing PAGE [50], which was run at 30 mA under high calcium conditions (100 μM free calcium in gel buffers) or low calcium conditions (1mM EGTA in gel buffers). Binding of CBD to CaM was visualized by Coomassie blue R-250 staining.

Fluorescence Spectroscopy

The steady-state flavin fluorescence was measured in a solution containing 25 mM Tris, pH 7.5, 100 mM NaCl, 0.1 mM DTT, 2 mM EGTA, 10% glycerol, and ~6 μM eNOS in the absence or presence of ~12 μM of CaM constructs using a VARIAN CARY Eclipse fluorescence spectrophotometer. A 1-ml quartz cuvette with a path length of 1 cm was used for the experiments. The total volume change was kept less than 0.3%, and the samples were maintained at room temperature during measurement. The effect of wild-type and mutant CaM binding on the eNOS flavin fluorescence was monitored upon addition of 2.5 mM $CaCl_2$. The protein was excited at 455 nm and emission spectra were recorded between 460 to 700 nm within 5 min for each sample. Emission spectra were corrected for background due to the buffer and CaM effects.

Trypsinolysis of eNOS

Limited proteolysis was carried out in a mixture containing 5 μM of recombinant eNOS purified from Sf21 cells, 50 mM Tris, pH 7.5, 100 mM NaCl, 10 μM of wild-type or mutant CaM, and either in the presence of 100 μM $CaCl_2$ or 1mM EGTA. Samples were preincubated at room temperature for 15 min, and proteolysis was initiated by addition of 0.1 ng of Trypsin Gold (Promega) per pmol of eNOS. Following incubation at room temperature for 15 min, the reaction was terminated by boiling with an equal volume of 2X SDS gel-loading buffer. Proteolytic

products were resolved on an 8–16% gradient SDS-PAGE [50] and visualized by staining with Coomassie Blue R250.

N-terminal sequence analysis

Following SDS-PAGE, the tryptic samples were transferred to polyvinylidene difluoride (PVDF) membranes using CAPS buffer for 3 h at 50 V and 4°C. The bands were stained with Ponceau red and excised for sequencing. Sequencing was performed on an Applied Biosystems Model 494 protein sequencer at Mission Biotech Inc. (Taipei, Taiwan).

Acknowledgments

The human CaM cDNA was a gift from Dr. Emanuel E Strehler.

Author Contributions

Conceived and designed the experiments: PFC. Performed the experiments: PRW. Analyzed the data: PFC PRW CCK. Contributed reagents/materials/analysis tools: CCK JYL. Wrote the paper: PFC KKW SFY.

References

1. Rafikov R, Fonseca FV, Kumar S, Pardo D, Darragh C, et al. (2011) eNOS activation and NO function: structural motifs responsible for the posttranslational control of endothelial nitric oxide synthase activity. J Endocrinol 210: 271–284.
2. Dudzinski DM, Michel T (2007) Life history of eNOS: partners and pathways. Cardiovascular Research 75: 247–260.
3. Schmidt HH, Wilke P, Evers B, Bohme E (1989) Enzymatic formation of nitrogen oxides from L-arginine in bovine brain cytosol. Biochem Biophys Res Commun 165: 813–819.
4. Bredt DS, Hwang PM, Glatt CE, Lowenstein C, Reed RR, et al. (1991) Cloned and expressed nitric oxide synthase structurally resembles cytochrome P-450 reductase. Nature 351: 714–718.
5. Stuehr DJ, Cho HJ, Kwon NS, Weise M, Nathan C (1991) Purification and characterization of the cytokine-induced macrophage nitric oxide synthase: an FAD- and FMN-containing flavoprotein. Proc Natl Acad Sci U S A 88: 7773–7777.
6. Xie QW, Cho HJ, Calaycay J, Mumford RA, Swiderek KM, et al. (1992) Cloning and characterization of inducible nitric oxide synthase from mouse macrophages. Science 256: 225–228.
7. Pollock JS, Förstermann U, Mitchell JA, Warner TD, Schmidt HH, et al. (1991) Purification and characterization of particulate endothelium-derived relaxing factor synthase from cultured and native bovine aortic endothelial cells. Proc Natl Acad Sci U S A 88: 10480–10484.
8. Sheta EA, McMillan K, Masters BS (1994) Evidence for a bidomain structure of constitutive cerebellar nitric oxide synthase. J Biol Chem 269: 15147–15153.
9. Ghosh DK, Stuehr DJ (1995) Macrophage NO synthase: characterization of isolated oxygenase and reductase domains reveals a head-to-head subunit interaction. Biochemistry 34: 801–807.
10. Chen PF, Tsai AL, Berka V, Wu KK (1996) Endothelial nitric-oxide synthase. Evidence for bidomain structure and successful reconstitution of catalytic activity from two separate domains generated by a baculovirus expression system. J Biol Chem 271: 14631–14635.
11. Abu-Soud HM, Yoho LL, Stuehr DJ (1994) Calmodulin controls neuronal nitric-oxide synthase by a dual mechanism. Activation of intra- and interdomain electron transfer. J Biol Chem 269: 32047–32050.
12. Siddhanta U, Presta A, Fan BC, Wolan D, Rousseau DL, et al. (1998) Domain swapping in inducible nitric-oxide synthase. Electron transfer occurs between flavin and heme groups located on adjacent subunits in the dimer. J Biol Chem 273: 18950–18958.
13. Sagami I, Daff S, Shimizu T (2001) Intra-subunit and inter-subunit electron transfer in neuronal nitric-oxide synthase: effect of calmodulin on heterodimer catalysis. J Biol Chem 276: 30036–30042.
14. Aoyagi M, Arvai AS, Tainer JA, Getzoff ED (2003) Structural basis for endothelial nitric oxide synthase binding to calmodulin. Embo J 22: 766–775.
15. Chen PF, Wu KK (2009) Two synthetic peptides corresponding to the proximal heme-binding domain and CD1 domain of human endothelial nitric-oxide synthase inhibit the oxygenase activity by interacting with CaM. Arch Biochem Biophys 486: 132–140.
16. Babu YS, Bugg CE, Cook WJ (1988) Structure of calmodulin refined at 2.2 A resolution. J Mol Biol 204: 191–204.
17. Wang CL (1985) A note on calcium binding to calmodulin. Biochem Biophys Res Commun 130: 426–430.
18. Meador WE, Means AR, Quiocho FA (1992) Target enzyme recognition by calmodulin: 2.4 A structure of a calmodulin-peptide complex. Science 257: 1251–1255.
19. Cho HJ, Xie QW, Calaycay J, Mumford RA, Swiderek KM, et al. (1992) Calmodulin is a subunit of nitric oxide synthase from macrophages. J Exp Med 176: 599–604.
20. Bredt DS, Snyder SH (1990) Isolation of nitric oxide synthetase, a calmodulin-requiring enzyme. Proc Natl Acad Sci U S A 87: 682–685.
21. Stevens-Truss R, Beckingham K, Marletta MA (1997) Calcium binding sites of calmodulin and electron transfer by neuronal nitric oxide synthase. Biochemistry 36: 12337–12345.
22. Gribovskaja I, Brownlow KC, Dennis SJ, Rosko AJ, Marletta MA, et al. (2005) Calcium-binding sites of calmodulin and electron transfer by inducible nitric oxide synthase. Biochemistry 44: 7593–7601.
23. Spratt DE, Taiakina V, Guillemette JG (2007) Calcium-deficient calmodulin binding and activation of neuronal and inducible nitric oxide synthases. Biochim Biophys Acta 1774: 1351–1358.
24. Govers R, Rabelink TJ (2001) Cellular regulation of endothelial nitric oxide synthase. Am J Physiol Renal Physiol 280: F193–F206.
25. Shifman JM, Choi MH, Mihalas S, Mayo SL, Kennedy MB (2006) Calcium/calmodulin-dependent protein kinase II (CaMKII) is activated by calmodulin with two bound calciums. Proc Natl Acad Sci USA. 103: 13968–13973.
26. Craig DH, Chapman SK, Daff S (2002) Calmodulin activates electron transfer through neuronal nitric-oxide synthase reductase domain by releasing an NADPH-dependent conformational lock. J Biol Chem 277: 33987–33994.
27. Ghosh DK, Salerno JC (2003) Nitric oxide synthases: domain structure and alignment in enzyme function and control. Front Biosci 8: 193–209.
28. Garcin ED, Bruns CM, Lloyd SJ, Hosfield DJ, Tiso M, et al. (2004) Structural basis for isozyme-specific regulation of electron transfer in nitric-oxide synthase. J Biol Chem 279: 37918–37927.
29. Roman LJ, Masters BS (2006) Electron transfer by neuronal nitric-oxide synthase is regulated by concerted interaction of calmodulin and two intrinsic regulatory elements. J Biol Chem 281: 23111–23118.
30. Li H, Das A, Sibhatu H, Jamal J, Sligar SG, et al. (2008) Exploring the electron transfer properties of neuronal nitric-oxide synthase by reversal of the FMN redox potential. J Biol Chem 283: 34762–34772.
31. Ilagan RP, Tiso M, Konas DW, Hemann C, Durra D, et al. (2008) Differences in a conformational equilibrium distinguish catalysis by the endothelial and neuronal nitric-oxide synthase flavoproteins. J Biol Chem 283: 19603–19615.
32. Lee A, Zhou H, Scheuer T, Catterall WA (2003) Molecular determinants of Ca(2+)/calmodulin-dependent regulation of Ca(v)2.1 channels. Proc Natl Acad Sci USA 100: 16059–16064.
33. Jama AM, Gabriel J, Al-Nagar AJ, Martin S, Baig SZ, et al. (2011) Lobe-specific functions of calcium calmodulin in α calcium calmodulin-dependent protein kinase II activation. J Biol Chem 276: 30794–30802.
34. Romanin C, Gamsjaeger R, Kahr H, Schaufler D, Carlson O, et al. (2000) Ca(2+) sensors of L-type Ca(2+) channel. FEBS lett 487: 301–306.
35. Tang W, Halling DB, Black DJ, Pate P, Zhang JZ, et al. (2003) Apocalmodulin and calcium calmodulin-binding sites on the CaV1.2 channel. Biophys J 85: 1538–1547.
36. Persechini A, McMillans K, Leakey P (1994) Activation of myosin light chain kinase and nitric oxide synthase activities by calmodulin fragments. J Biol Chem 269: 16148–16154.
37. Adak S, Ghosh S, Abu-Soud HM, Stuehr DJ (1999) Role of reductase domain cluster 1 acidic residues in neuronal nitric-oxide synthase. Characterization of the FMN-FREE enzyme. J Biol Chem 274: 22313–22320.
38. Salerno JC, Harris DE, Irizarry K, Patel B, Morales AJ, et al. (1997) An autoinhibitory control element defines calcium-regulated isoforms of nitric oxide synthase. J Biol Chem 272: 29769–29777.
39. Liu J, Sessa WC (1994) Identification of covalently bound amino-terminal myristic acid in endothelial nitric oxide synthase. J Biol Chem 269: 11691–11694.
40. Liu J, Garcia-Cardeiia G, Sessa WC (1995) Biosynthesis and palmitoylation of endothelial nitric oxide synthase: mutagenesis of palmitoylation sites, cysteines-15 and/or -26, argues against depalmitoylation-induced translocation of the enzyme. Biochemistry 34: 12333–12340.
41. Haque MM, Koustubh P, Tejero J, Aulak KS, Fadlalla MA, et al. (2007) A connecting hinge represses the activity of endothelial nitric oxide synthase. Proc Natl Acad Sci U S A 104: 9254–9259.
42. Xia C, Misra I, Iyanagi T, Kim JJ (2009) Regulation of interdomain interactions by calmodulin in inducible nitric-oxide synthase. J Biol Chem 284: 30708–30717.
43. Tejero J, Haque1 MM, Durra D, Stuehr DJ (2010) A bridging interaction allows calmodulin to activate NO synthase through a bi-modal mechanism. J Biol Chem 285: 25941–25949.
44. Daff S (2010) NO synthase: structures and mechanisms. Nitric Oxide 23:1–11.
45. Rodney GG, Krol J, Williams B, Beckingham K, Hamilton SL (2001) The carboxy-terminal calcium binding sites of calmodulin control calmodulin's Switch from an Activator to an Inhibitor of RYR1. Biochemistry 40: 12430–12435.

46. Newman E, Spratt DE, Mosher J, Cheyne B, Montgomery HJ, et al. (2004) Differential activation of nitric-oxide synthase isozymes by calmodulin-troponin C chimeras. J Biol Chem 279: 33547–33557.
47. Chen PF, Tsai AL, Wu KK (1994) Cysteine 184 of endothelial nitric oxide synthase is involved in heme coordination and catalytic activity. J Biol Chem 269: 25062–25066.
48. Pitt GS, Zűhlke RD, Hudmon A, Schlman H, Reuter H, et al. (2001) Molecular basis of calmodulin tethering and calcium-dependent inactivation of L-type calcium channels. J Biol Chem 276: 30794–30802.
49. Bradford MM (1976) A rapid and sensitive method for the quantitation of microgram quantities of protein utilizing the principle of protein-dye binding. Anal Biochem 72: 248–254.
50. Laemmli UK (1970) Cleavage of structural proteins during the assembly of the head of bacteriophage T4. Nature 227: 680–685.